Development of a multi-zone irradiation model for scenario studies involving ASTRID-like SFRs

Léa Tillard, Jean-Baptiste Clavel, Xavier Doligez, Eric Dumonteil, Marc Ernoult, Florian Mang, Abdoul-Aziz Zakari-Issoufou

ICAPP 2019 – International Congress on Advances in Nuclear Power Plants
France, Juan-les-pins – 2019, May 12 │15

Development of a multi-zone irradiation model for scenario studies involving ASTRID-like SFRs

Léa Tillard[1*], Jean-Baptiste Clavel[1], Xavier Doligez[2], Éric Dumonteil[1], Marc Ernoult[2], Florian Mang[1], Abdoul-Aziz Zakari-Issoufou[2]

[1]IRSN, PSN-EXP/SNC/LN, Fontenay-aux-Roses, France
[2]IPNO, CNRS-IN2P3/Univ. Paris Sud, Orsay, France
[*]Corresponding Author, E-mail: lea.tillard@irsn.fr

Abstract: The French 600 MWe Sodium-cooled Fast Reactors with "low void effect" (SFR-CFV) ASTRID is a highly heterogeneous reactor design composed of several fissile and fertile fuel zones. It can be operated as plutonium break-even or burner. This paper presents an exploration of both behaviors for many different fresh fuel compositions built from UOX and MOX spent fuels. It will show that the plutonium content as well as the fresh fissile fuel isotopic vector are the two parameters strongly affecting the fuel composition evolution during irradiation. Consequently, for fuel cycle prospective studies involving such SFR integrated into a Pressurized Water Reactors (PWR) fleet, it is required to use simulation codes with an ad hoc fuel irradiation model able to maintain the core heterogeneity during the depletion calculation while keeping the interactions between the different fuel zones. This new model was implemented in the dynamic fuel cycle simulation tool CLASS and is based on two predictors used to estimate, per zone, mean cross-sections and flux values. The good accuracy of this new model on plutonium and minor actinides inventories may also allow physical data important for safety assessment of fuel cycle to be estimated and transmutation scenario studies integrating potential fissile and fertile separation.

KEYWORDS: ASTRID, Sodium-cooled Fast Reactor, Irradiation model, Fuel Cycle

I) Introduction and motivations

Several countries explore the possible deployment of SFR. In France, the evolution of the electronuclear fleet for the next years is not fully defined yet and the progressive deployment of so-called SFR-CFV is one of the potential strategies considered (1). Different options are envisaged regarding the agenda for the deployment time of this kind of reactors, depending on the global nuclear energy development and the national energy mix strategies. One way to analyze and compare different possible options relies on scenario studies using dynamic fuel cycle simulation codes. These codes calculate amongst other the fuel composition evolution in all reactors for each cycle during the whole defined scenario. Moreover, fuel cycle studies evaluate isotopic compositions in all the involving radioactive materials. These studies therefore allow to estimate physical data important for safety assessment of fuel cycle such as heat, neutron and gamma doses… In this context, the underlying goal of the work presented here is to perform scenarios involving SFR-CFV within a PWR fleet with the code CLASS.

The SFR-CFV core studied in this paper, called ASTRID-like SFR, is based on the 600 MWe French CFV-V1 ASTRID concept developed by the CEA and its industrial partners (2). This reactor concept has gathered attention for its flexibility as it can operate as a plutonium breeder, break-even or burner. In this work, only the break-even and the burner configurations are studied; the latest design has been obtained by modifying the first one thanks to work carried out at KIT (3).

This paper presents in part II) some ASTRID-like properties depending on possible fresh fuel compositions. From this study, a numerical model of the reactor evolution, presented in part III), is built to be included in the CLASS code (4; 5). The accuracy of this new model is then analyzed in the following parts.

Maintaining a negative void coefficient all along the cycle time of this reactor is one of the typical SFR challenges. To overcome it, the ASTRID designs are strongly heterogeneous. The break-even core is divided in two radial parts: an inner and an outer core, both of them axially divided in fertile and fissile

zones. The plutonium production in the fertile zones compensate the disappearance in the fissile zones, hence the plutonium equilibrium is assured. This axial division and the crenel shape are important differences with the European SFR concept (6). The geometry is designed to increase neutron leakage especially in case of sodium void in some parts of the core (7). Hence, there are six fuel zones in the ASTRID-like break-even design as shown on Figure 1. Zone 1 is the upper fissile zone, zone 2 the inner fertile zone, zone 3 the lower fissile zone, zone 4 the inner fertile blanket, zone 5 the external fissile zone and zone 6 is the outer fertile blanket.

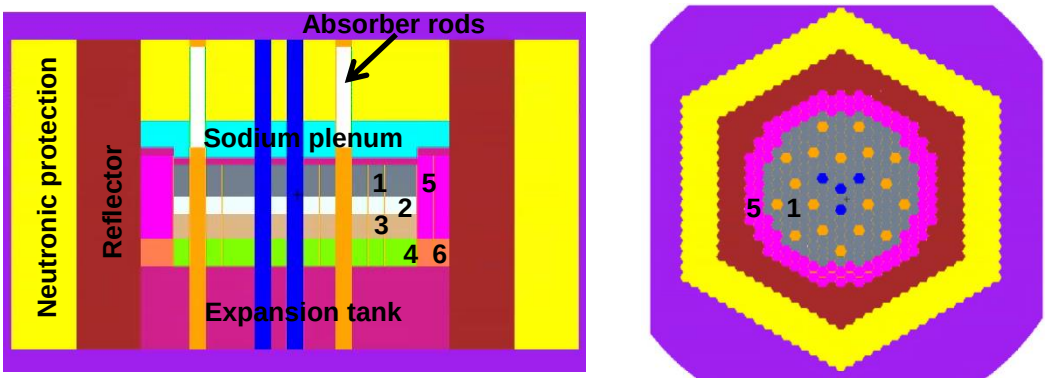

Figure 1: Axial (on the left) and radial (on the right) layouts of ASTRID-like break-even core

In the burner concept, the goal is to decrease the breeding ratio. Consequently, to prevent plutonium production, fertile zones have been removed from the core, as shown in Figure 2. Power and dimensions of this burner design have been reduced to maintain the same power density as in the break-even design. Hence, only two fissile fuel zones are left. Zone 1 is the internal fissile zone and zone 2 is the external fissile zone.

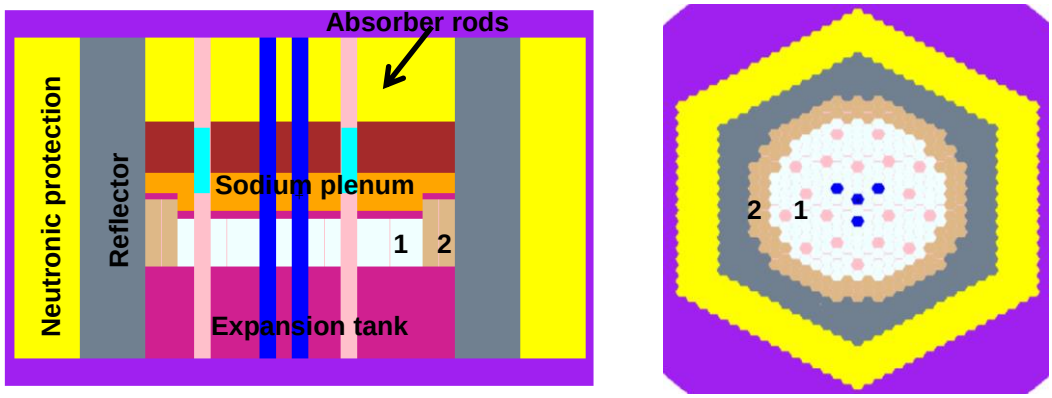

Figure 2: Axial (on the left) and radial (on the right) layouts of ASTRID-like burner core

The role of each of these zones in the reactor changes during the depletion. Figure 3 shows the evolution of powers per zone as a function of the global reactor burnup evolution for the break-even core entirely loaded with the “reference” fresh fuel presented in Table 1 (2). This simulation is a full core depletion calculation made with the VESTA code (8), which allows a coupling between its native depletion solver PHOENIX and the MCNP6 Monte Carlo neutron transport code (9). At the Beginning Of Cycle (BOC) state, all the fertile zones produce less than 5% of the total reactor power. However, during irradiation up to 100 GWd/t_{HM}, global reactor burnup, the inner fertile zone and fissile zones become comparable in terms of power production. At the End Of Cycle (EOC) step, the inner fertile zone produces around 15% of the reactor power matching the upper fissile zone.

Hence, the behavior of the fuel evolution of each zone is strongly dependent on the different initial fissile fuel compositions. The goal of this work is to simulate scenarios integrating ASTRID-like SFR cores within a PWR fleet. These cores are loaded with a priori unknown fuel, which composition depends on many parameters of the scenario such as recycling choices, PWR burnups, cooling time... Thus, a deeper look into the impact of the different fuel compositions on ASTRID-like behavior's evolution is required before the development of a new dedicated irradiation model in the CLASS code.

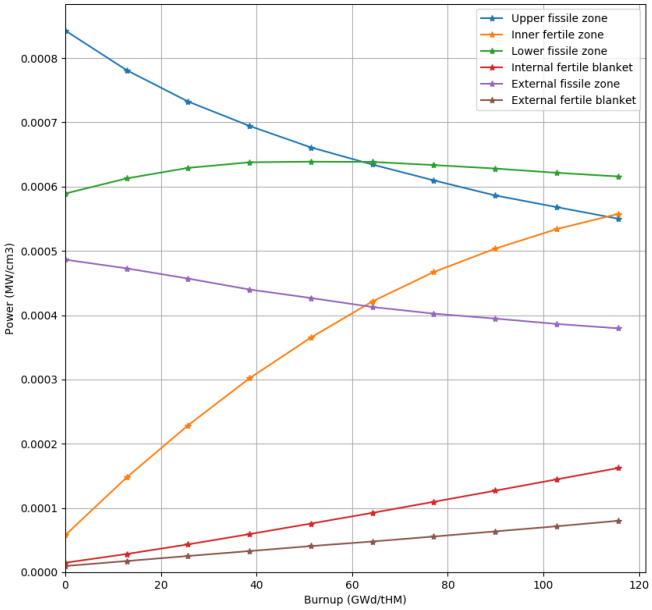

Figure 3: Evolution of the fuel zone's powers (in MW/cm^3) during irradiation for the break-even core

	Internal core / External core
Isotope	(%)
^{238}Pu	2.59 / 2.59
^{239}Pu	55.2 / 55.2
^{240}Pu	25.85 / 25.85
^{241}Pu	7.27 / 7.27
^{242}Pu	7.57 / 7.57
^{241}Am	1.22 / 1.22
TPu	23.52 / 20.02

Table 1: Isotopic proportions and Pu contents (TPu) for the break-even core

II) Evolution of ASTRID-like behavior during irradiation

In the scenario studies considered in this work, ASTRID-like SFR may be loaded with plutonium coming from PWR loaded with UOX or MOX fuels. Moreover, PWR spent fuels may have cooled during a long period before being reprocessed to recycle the plutonium in ASTRID-like reactors. Hence, to be representative this study has to cover the possible fresh SFR's fuels that may appear during the scenario. Each isotopic proportion ranges are determined based on the following considerations (10):

- UOX spent fuel irradiated in PWR up to 33 GWd/t_{HM}, then cooled for 3 years,
- UOX spent fuel irradiated in PWR up to 47.5 GWd/t_{HM}, then cooled for 5 years,
- MOX spent fuel irradiated in PWR up to 43.5 GWd/t_{HM}, then cooled for 4 years.

Both the reactor burnups and the cooling time affect the plutonium isotopic composition. Furthermore, before partitioning, these three spent fuel compositions may be stored over different periods going from 2 to 100 years, slightly different periods have been considered for the two designs. Finally, wide plutonium content variation ranges are chosen for internal and external core. Ranges obtained are presented in Table 2.

Isotope		^{238}Pu	^{239}Pu	^{240}Pu	^{241}Pu	^{242}Pu	^{241}Am	^{242m}Am	^{243}Am	TPu_int	TPu_ext
Break-even	Min (%)	1	3	20	0	5	0	-	-	15	15
	Max (%)	8	74	40	17	17	15	-	-	40	40
Burner	Min (%)	0	3	18	0	3	0	1	1	15	15
	Max (%)	7	79	32	17	15	20	5	5	40	40

Table 2: Ranges used for fresh fuel considered in the ASTRID-like study

In order to quantify the impact of the initial plutonium isotopic composition on the reactors properties, a thousand depletion calculations are performed. The different initial fissile compositions are sampled by the Latin Hypercube Sampling method (11) inside the ranges presented in Table 2. The sampling method leads to some unrealistic compositions but assure that all possible one is covered. Fertile fresh fuel composition is always depleted uranium containing 0.2% of ^{235}U. For the break-even design, the upper and lower internal fissile fresh fuel differ only by their volume. The burner reactor is here

designed to burn only plutonium followed by americium; therefore other minor actinides are not put in fresh fuel. Table 3 shows some mean statistical uncertainties at EOC for the break-even core loaded with the "reference" fuel, Table 1, considering either all fuel zones or only fertile blankets. Uncertainties in fertile blankets appear to be dominant for all quantities of interest in depletion calculations.

Quantity of interest	$\sigma_{f,^{239}Pu}$	$\sigma_{c,^{239}Pu}$	$\sigma_{n2n,^{239}Pu}$	$\sigma_{f,^{241}Pu}$	φ	$N_{^{239}Pu}$
All fuel zones (%)	0.7	1.7	8.5	0.7	1.9	0.3
Only fertile blankets (%)	1.6	3.6	16.3	1.3	2.4	0.7

Table 3: Mean statistical uncertainties for some quantities of interest at EOC for the break-even core

Figure 4 (a) shows a histogram of all the 1000 multiplication factors calculated at BOC for the break-even configuration. The depletion calculations are also performed for under critical configurations. Thus, some of the different values are clearly not acceptable and this plot shows the necessity to take into account the initial reactivity to build the fresh fuel, i.e. to adapt the plutonium content to reach a given reactivity for the fresh fuel. Figure 4 (b) shows the reactivity evolution during the irradiation campaign that is always smaller than 4000 pcm, i.e. the order of magnitude for control rods worth for this kind of reactors. This figure shows that the reactivity evolution is consequently not a parameter of importance for fresh fuel considerations.

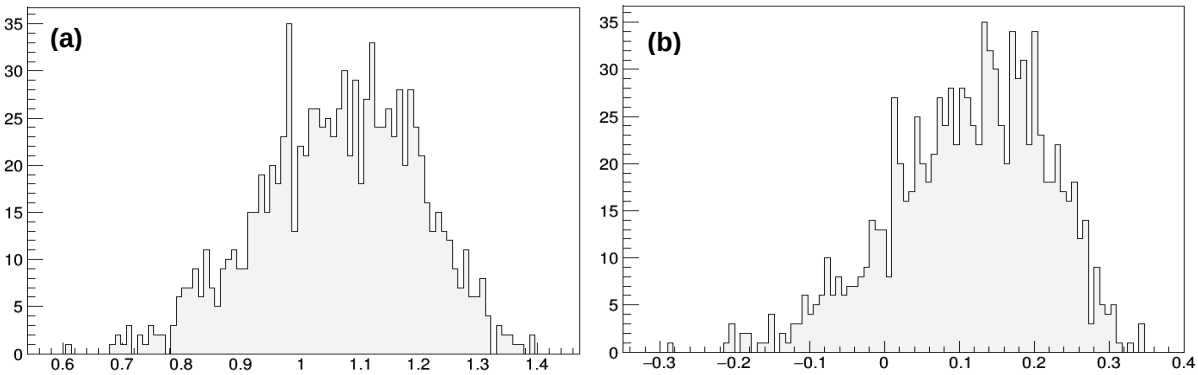

Figure 4: Histogram for the 1000 evolutions of (a) k_{eff} distribution at BOC and (b) reactivity variations during irradiation, in both cases for the break-even core

Figure 5 shows the global variation of plutonium for the 1000 depletion calculations. It represents the plutonium consumption or the production, in %, as a function of the irradiation time and clearly shows that the behavior of the fuel depends on the fresh fuel composition.

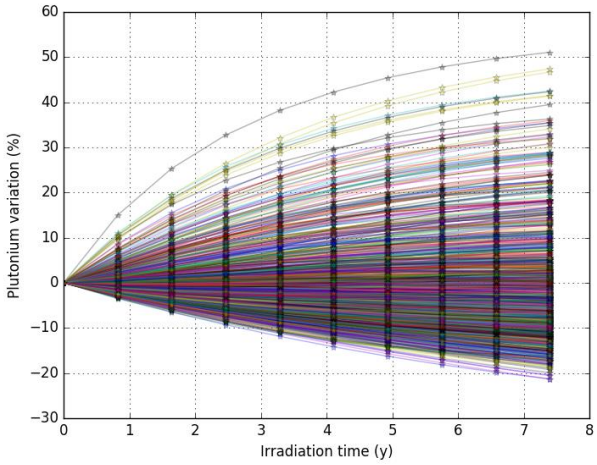

Figure 5: Variation of global plutonium inventory over time for the 1000 depletion calculations of the break-even configuration

Finally, the fuel evolution, as its isotopic quality, is strongly dependent of the fresh fuel composition. The plutonium content in such a fuel has to be adapted to the plutonium isotopic composition used to load the reactor. Both of the plutonium content and its isotopic vector impact strongly the evolution, and consequently the SFR spent fuel composition. For fuel cycle prospective studies, it is then necessary to build fabrication and irradiation models representative of the ASTRID-like reactor physics.

As ASTRID-like SFR fuel zone behavior varies a lot, the development in the CLASS code of a new fuel irradiation model, related to ASTRID and its multi-zone fuel loading plan is needed for scenario studies involving this kind of reactors. This new model, described in the next section, aims at maintaining the core heterogeneity during the depletion calculation while keeping the interactions between the different fuel zones during evolution.

III) The multi-zone irradiation model

The isotopic fuel evolution during irradiation in an operating reactor is described by the Bateman Equation 1:

$$\frac{dN_i}{dt} = -(\lambda_i + \sigma_i \times \varphi)N_i + \sum_{j \neq i}\left(\lambda_{j\to i} + \sigma_{j\to i} \times \varphi\right) N_j \qquad \textbf{Equation 1}$$

where N_x represents the number of nucleus x, λ_x is the radioactivity decay constant of isotope x, σ_x is the total absorption cross-section of the nucleus x and φ the neutron flux in the system. In the CLASS code, current irradiation models solve the Bateman Equation 1 considering only fission, capture and (n,2n) reactions at reactor level (12), that is to say considering an homogeneous fuel. As mentioned in the part II), ASTRID-like SFR are strongly heterogeneous and such a global model would not be able to render its spatial complexity, leading us to develop a multi-zone model.

In the multi-zone irradiation model, the equations are solved for each zone z, knowing the cycle time of the reactor and all the initial fuel compositions. Equation 1 becomes then Equation 2 where $\sigma_{x,z}$ and φ_z are local. In zone z, the flux is linked to the power P_z, as described in Equation 3 where ${\varepsilon_i}^{fis}$ is the mean fission energy and ${\sigma_{i,z}}^{fis}$ the fission cross-section in zone z.

$$\left.\frac{dN_i}{dt}\right]_z = -\left(\lambda_i + \sigma_{i,z} \times \varphi_z\right)N_{i,z} + \sum_{j \neq i}\left(\lambda_{j\to i} + \sigma_{j\to i,z} \times \varphi_z\right) N_{j,z} \qquad \textbf{Equation 2}$$

$$\varphi_z(t) = \frac{P_z(t)}{\sum_i {\varepsilon_i}^{fis} \times {\sigma_{i,z}}^{fis}(t) \times N_{i,z}(t)} \quad \text{with} \quad P_{tot} = \sum_z P_z(t) \qquad \textbf{Equation 3}$$

To solve Equation 2, average cross sections and the flux value are needed for each zone. All the local values, cross-sections and flux or powers, depend on the fuel composition of all zones at each time step. They are a priori unknown. The multi-zone irradiation model uses two independent predictors based on artificial neural networks to calculate these local values, cross-sections and flux, quickly and reliably. Neural networks used here are Multi-Layer Perceptrons (MLP). As in previous models in the CLASS code, they are provided by the TMVA library of ROOT (13). Each MLP is trained on a training database as explained in previous work done by the CLASS community (14).

MLP input parameters are, in this work, time, fissile fresh fuel compositions and zone number. However, the power predictor has an additional constraint. In fact, as depicted in Equation 3, the sum of all powers per zone must be kept equal to the reactor power and then local power prediction must be renormalized. Effects of reactor heterogeneity are maintained through the zone number parameter and the initial fissile inventories bound the different fuel evolution of the global core. This spatial discretization is a new parameter for irradiation models in the code CLASS.

Training databases in this study are composed of 1000 full core depletion calculations made with the VESTA code and differing only by their fissile fresh fuel compositions, as in the section II). Isotopic proportion ranges are presented in Table 2. Using the same ranges, independent testing databases are generated to verify predictor accuracy. They are composed of 200 full core depletion calculations providing Monte Carlo results taken as a reference for the precision verification. Each depletion calculation, without task parallelization, lasts about 42 days for a single processor.

So this new multi-zone irradiation model's utilization is based on a multi-zone Cross-Section Predictor (CSP) and either a local Power Predictor (PP) or a local Flux Predictor (FP).

IV) Cross-section predictors (CSP)

The CSP aims at predicting the average cross-section per zone for fission, capture and (n,2n) reactions of all isotopes. One independent MLP per cross-section to be predicted is used. Predictors' accuracy is verified using the testing database. Values of the database are then taken as a reference and compared with the MLP predictions through Equation 4, where r is one of the three reactions, i the isotope of interest and z the fuel zone.

$$D\sigma_{r,i,z} = \left| \frac{{\sigma_{r,i,z}}^{VESTA} - {\sigma_{r,i,z}}^{CLASS}}{{\sigma_{r,i,z}}^{VESTA}} \right| \qquad \textbf{Equation 4}$$

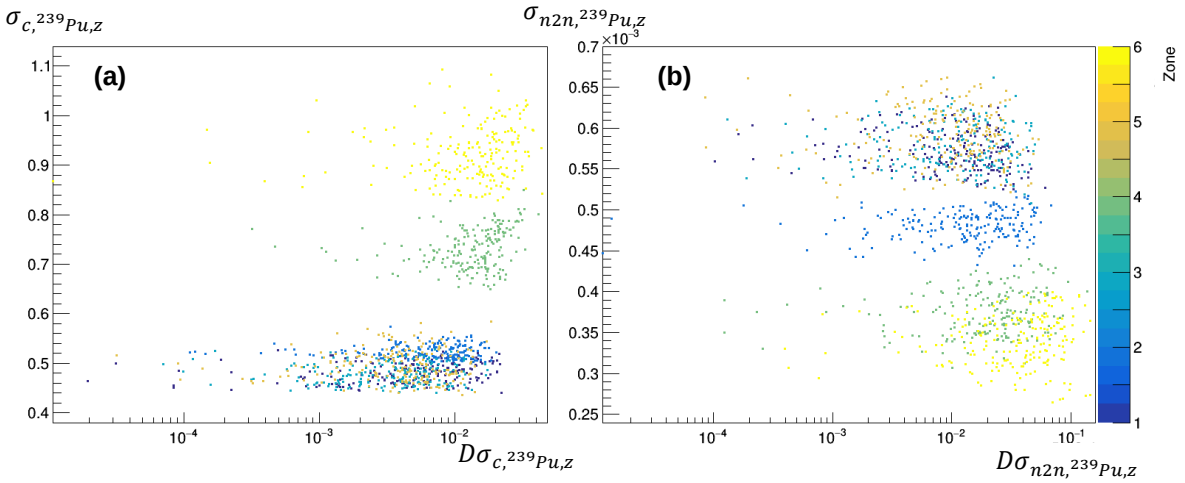

Figure 6: Comparison between VESTA and CSP calculation (a) of ^{239}Pu capture cross-section and (b) of ^{239}Pu (n,2n) cross-section per zone at EOC for the break-even design

Figure 6 depicts respectively the induced errors on ^{239}Pu capture (a) and (n,2n) (b) cross-sections at EOC, per zone, for the break-even reactor. The ordinate axis is the Monte Carlo value in barns while the abscissa is the predictor's induced deviation. Here each color represents one fuel zone and each point is one of the 200 simulations from the break-even testing database. Capture reaction error is lower than 4%, thus, it has the same magnitude order as the mean statistical uncertainty from depletion calculation, Table 3. Because (n,2n) reactions are threshold reactions, errors are higher than for capture or fission cross-section but still error stays lower than 10%. Statistics in fertile zones, especially in the fertile blankets, i.e. zone 4 and 6, are also lower due to low flux values, hence, predictors' errors are higher than in the fissile zones or in the inner fertile zone, i.e. zone 1, 2, 3 and 5.

Figure 7 represents induced errors on fission cross-sections for ^{239}Pu (a) and ^{241}Pu (b) at EOC per zone for the break-even reactor. Again, errors in fertile blankets are dominant, but lower than 2%, thus the same order of magnitude as statistical uncertainty, Table 3. Hence, numerical improvement will not be realistic. As shown in Equation 2, errors induced by the CSP have an impact on inventory evolutions. This effect is even more important for fission cross-sections as they have also a direct impact on flux calculation, when determined using the PP, Equation 3. Thus, fission cross-section predictors' induced errors have a double impact on final inventories.

For the burner design, similar results are observed. For instance, deviations at EOC per zone are respectively always lower than 0.3% for ^{239}Pu fission cross-sections and than 1% for ^{239}Pu capture cross-sections. Hence, results are satisfying as CSP induced errors and statistical uncertainties have the same magnitude order.

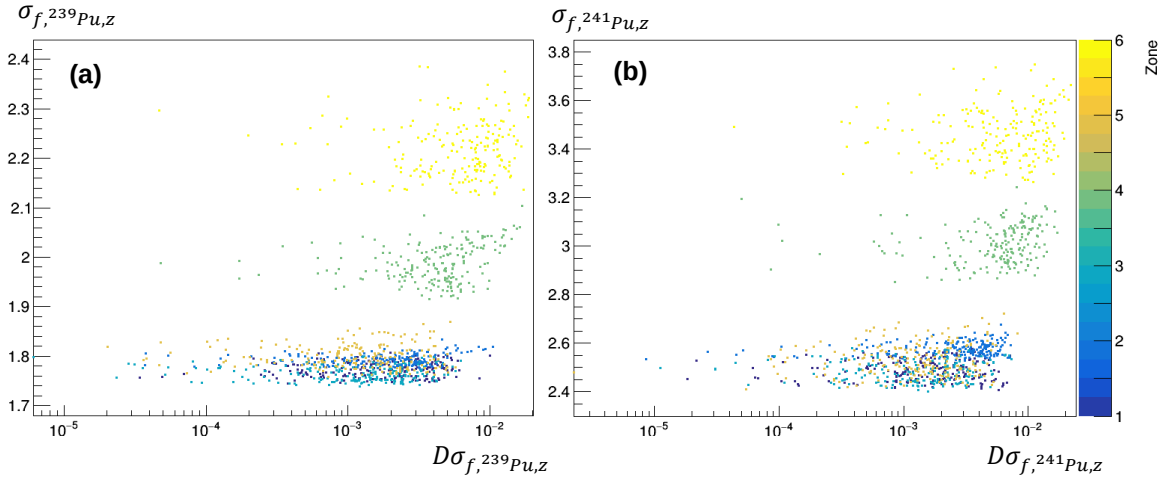

Figure 7: Comparison between VESTA and CSP calculation (a) of ^{239}Pu fission cross-section and (b) of ^{241}Pu fission cross-section per zone at EOC for the break-even design

V) Flux and Power predictors (FP and PP)

As seen in part III), flux per zone may be either predicted by the FP or calculated using the PP result. PP and FP are trained on the same training database as the CSP and take the same input parameters with an additional constraint for the PP explained in part III). Again, predictors' accuracy is checked on the testing database. Deviation is calculated with Equation 5 where X_z is either the percentage of total power produce by the fuel zone z or the local flux of zone z in cm^{-2}.s^{-1}.

$$DX_z = \left|\frac{X_z{}^{VESTA} - X_z{}^{CLASS}}{X_z{}^{VESTA}}\right| \qquad \textbf{Equation 5}$$

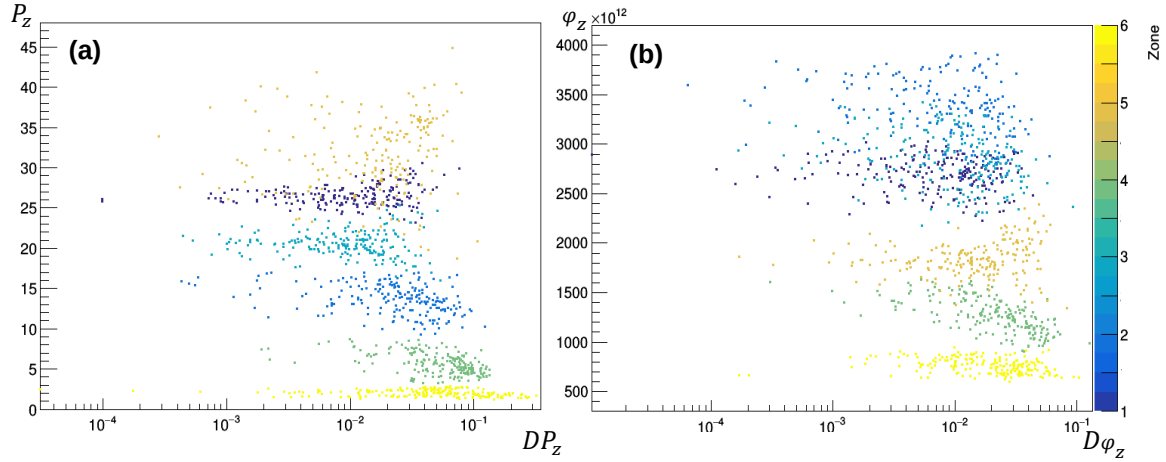

Figure 8: Comparison between VESTA and (a) PP predictions and (b) FP predictions per zone at EOC for the break-even design

Figure 8 (a) shows errors induced by the power predictor per zone at EOC for the break-even reactor. Ordinate values come from Monte Carlo simulations while deviations are in abscissa. Fissile zones in ASTRID-like reactor are responsible for the main part of the power production. At EOC, the inner fertile zone behavior is closed to a fissile zone in terms of power production. Deviations in these zones are lower than 7%. Errors induced by the PP in fertile blankets are dominant, higher of one magnitude order, reaching 30% at maximum. Prediction precision directly impacts flux calculation and composition estimation per zone. However, as fertile blankets represent a lower percentage of the total reactor power, power prediction error's impact should be balanced on a reactor scale.

Figure 8 (b) shows induced errors on flux per zone at EOC for the break-even reactor. Ordinate values, in cm-2.s-1, come from Monte Carlo simulations while deviations are in abscissa. Induced errors on local flux in fertile blankets are slightly dominant but lower than 7%. Fissile and inner fertile zones

induced errors are around 4% at maximum with errors of the same magnitude order for all fuel zones. The direct prediction of local flux leads to a noticeable improvement because it removes fission cross-sections and isotopic fissile compositions uncertainties into flux calculation. However, errors are not negligible and still impact final composition estimation per zone. Besides, reactor size and power's modulations get more challenging when using the FP. In fact, those parameters are usually controlled through the Equation 3, which does not intervene in the process when the FP is used.

For the burner design, as there are only fissile zones, local power deviations at EOC are comparable with errors induced in break-even fissile zones: errors stay under 2%. For the break-even reactor, independently of the method used to determine the flux per zone, major errors are observed into fertile blankets. They are suspected to be due to a lack of statistic in fertile areas during the Monte Carlo simulations. Two options are currently under investigation: increasing the total number of simulated neutrons during the training data-base generation or biasing fertile zone statistics using variance reduction methods.

VI) Complete depletion model

Once cross-sections per zone are estimated and flux determined either with the FP or with the PP, the evolution of isotopic quantities may be calculated by the multi-zone irradiation model presented in part III). To evaluate the precision of the model, EOC fuel compositions are estimated using the testing database. Then, deviations on inventories per zone between the CLASS code model and the reference values are calculated with the Equation 6 where $N_{i,z}$ is the quantity in atomic proportion of isotope i in zone z.

$$DN_{i,z} = \left| \frac{{N_{i,z}}^{VESTA} - {N_{i,z}}^{CLASS}}{{N_{i,z}}^{VESTA}} \right| \qquad \textbf{Equation 6}$$

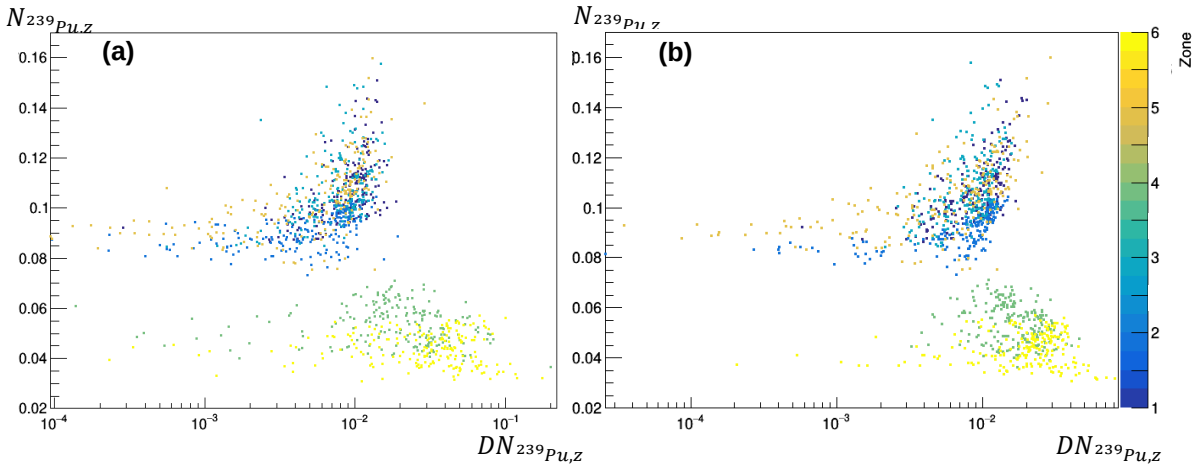

Figure 9: Comparison between VESTA and the multi-zone irradiation model using (a) PP predictions and (b) FP predictions for ^{239}Pu per zone at EOC for the break-even design

Figure 9 shows induced errors on ^{239}Pu inventory per zone at EOC for the break-even reactor respectively when using the PP or the FP. The ordinate axis is here $N_{i,z}$ divided by the total isotopic quantity in zone z. Maximum errors in fissile zones and the inner fertile zone are similar, around 1% in both case. However, the impact of intermediate predictors is visible in fertile blankets. As expected, a gain of a factor two on the ^{239}Pu estimation precision is noticeable, while using the FP instead of the PP. Deviations with the PP reach 10% while these values are around 5% with the FP.

Figure 10 presents the same graph than Figure 9 for the burner reactor. The two deviation branches for errors higher than 0.1% may be correlated with the two plutonium contents. Independently of intermediate predictors, errors on ^{239}Pu inventory at EOC are lower than 1%. Therefore, the multi-zone irradiation model gives very accurate result for reactor without fertile zone.

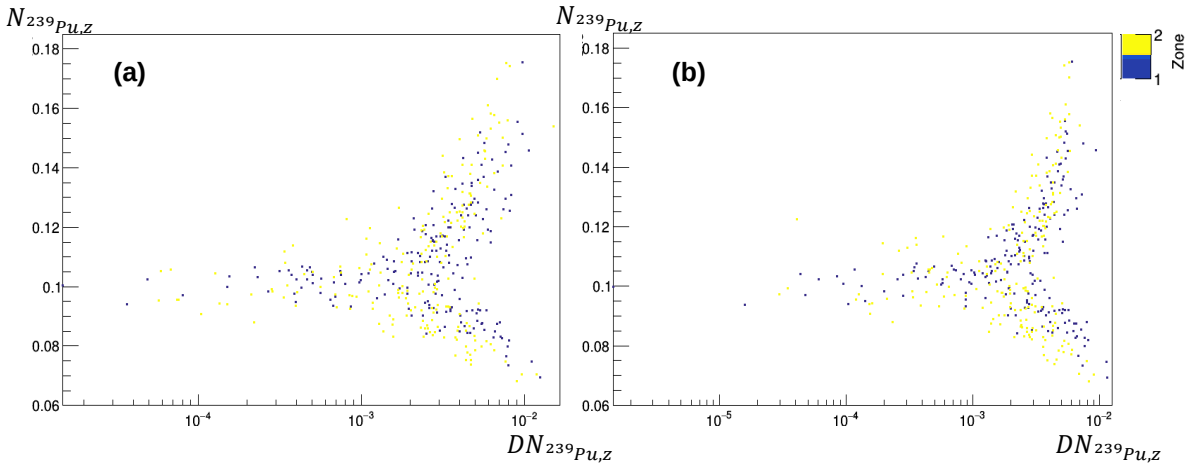

Figure 10: Comparison between VESTA and the multi-zone irradiation model using (a) PP predictions and (b) FP predictions for ^{239}Pu per zone at EOC for the burner design

Results per zone may be transformed to represent the global inventories. According to the fuel cycle scenario studied, knowing the fuel composition per zone in reactor can be less significant. For instance, if after the fuel evolution in reactor, fuels coming from different zones are recycled together. In that case, Equation 6 becomes Equation 7.

$$DN_{i,norm} = \left| \frac{\sum N_{i,z}^{VESTA} - \sum N_{i,z}^{CLASS}}{\sum N_{i,z}^{VESTA}} \right| \qquad \textbf{Equation 7}$$

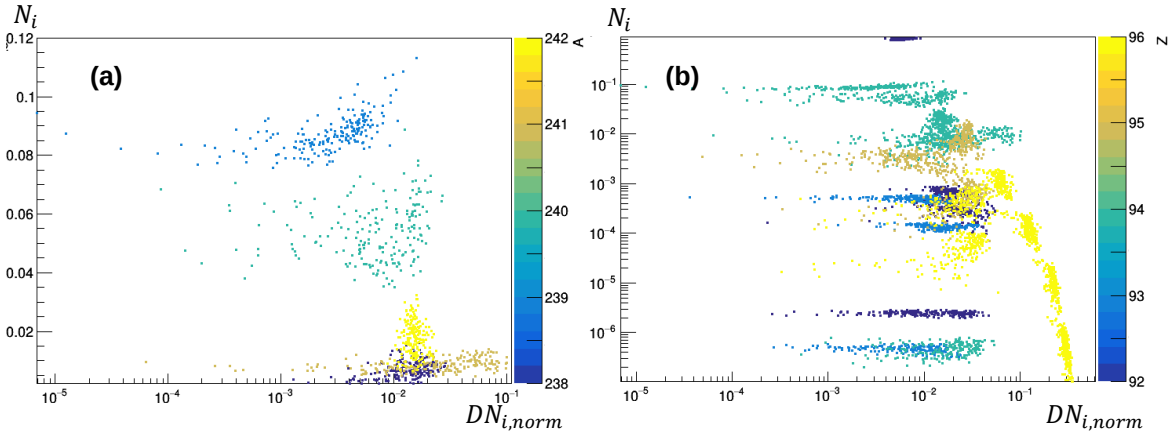

Figure 11: Comparison between VESTA and the multi-zone irradiation model using FP predictions for (a) Pu isotopes and (b) minor actinides at reactor level at EOC for the break-even design

Figure 11 presents induced errors on global plutonium (a) and minor actinide (b) inventories estimation at EOC for the break-even design using the FP. The ordinate axis is the total atomic proportion of plutonium or minor actinide of interest. Each color describes either one isotope of plutonium or one minor actinide element. The impact of fertile zone imprecision is balanced on a reactor scale as shown on Figure 11 (a). In fact, for plutonium isotopes, except for ^{241}Pu, induced errors are lower than 2% which is reliable enough for scenario simulations. It reaches 10% for ^{241}Pu. In fact, disappearance of ^{241}Pu is driven by a competition between decay and capture, while its production is only due to capture. So, because of the decay term, the equilibrium between production and disappearance depend on the flux value unlike other actinides.

However, Figure 11 (b) shows that even if results are satisfying for uranium, neptunium, plutonium and americium elements, errors on curium are higher and can flirt with 20% for some isotopes. However, curium isotopes associated with deviations superior as 10% represent less than 0.01% of the reactor's fuel. Results for the global inventories are similar when the PP is used. The relatively good accuracy of americium inventory may allow us to use this model for transmutation scenario. For the burner design, similar results are observed. For instance, deviations for plutonium isotopes at EOC stay below 2% and for americium isotopes below 3%.

These two graphs raise the question of adequacy of this new model with specific fertile separation and minor actinides multi-recycling in current state. This last point should be improved for MLP generated on new isotope ranges. Then, with the FP, results seem to be satisfying for plutonium multi-recycling and fissile separation.

VII) Conclusion

In this paper we discussed a methodology to deal with scenarios studies implying the use of ASTRID-like SFR reactors within a PWR fleet. ASTRID-like design is strongly heterogeneous, alternating several fissile and fertile fuel zones and allowing to operate them as plutonium break-even or burner. This work highlights that each fuel zone behavior highly depends on plutonium contents and isotopic vector of the fresh fissile fuels. Consequently, dedicated irradiation and fabrication models are needed in the CLASS code. This paper presents the new multi-zone irradiation model developed to reliably describe the fuel composition evolution of such reactors in a few minutes for fuel cycle prospective studies.

This new multi-zone model is based on two predictors used to estimate, per zone, the mean cross-sections and either the flux values or the power values. For all predictors, precision is better in fissile zones, where statistic of the depletions simulations is higher. However, for the break-even design, CSP induced deviations stay lower than 4% for plutonium fission and capture cross-section. PP induced errors stay below 10 %, while uncertainties are divided by a factor two thanks to the FP. Then, for the burner design, all predictors induce smaller deviations than for the break-even design. Finally, errors on plutonium inventories per zone, using the FP are satisfying enough to allow fissile and fertile separation in scenario studies integrating ASTRID-like SFR. Besides, on global compositions at EOC state, plutonium and major minor actinides deviations always stay below 10%. So transmutation scenario simulation using this new model is acceptable.

In conclusion, a simple scenario UOX-MOX-ASTRID using this new model has been simulated with CLASS to evaluate the impact of one break-even ASTRID reactor on plutonium isotopic quality. The scenario lasts 170 years, ASTRID-like reactor starts after 100 years. Burnups are for UOX 40 GWd/t_{HM}, for MOX 45 GWd/t_{HM} and 100 GWd/t_{HM} for ASTRID-like reactor. As a first approximation, no adaptive fabrication model is used for SFR, ASTRID-like plutonium contents stay equal to the values presented in (2). Before SFR starting time, plutonium isotopic vector in the spent MOX fuel storage is calculated. There is 47.6% of ^{239}Pu. Then, at EOC the same estimation is made in the spent ASTRID-like fuel storage. There is 57.9% of ^{239}Pu. Thus, the plutonium isotopic vector's quality is improved thanks to ASTRID-like break-even. Now more complex scenarios are targeted using both multi-zone fabrication and irradiation models.

References

(1) Direction de l'Energie Nucléaire du CEA*, Avancées des recherches sur la séparation-transmutation et le multi-recyclage du plutonium dans les réacteurs à flux de neutrons rapides*, Technical Report (2015)
(2) O.Fabbris, *Optimisation multi-physique et multicritère des cœurs RNR-Na : application au concept CFV*, Ph.D. Thesis in French, Université de Grenoble, France (2014)
(3) F. Gabrielli and al., *ASTRID-like Fast Reactor Cores for Burning Plutonium and Minor Actinides*, INES-4 (2015)
(4) B. Mouginot, and al., *Core library for advanced scenario simulation, CLASS: principle & application,* PHYSOR (2014)
(5) B. Leniau and al. *A neural network approach for burn-up calculation and its applications to the dynamic fuel cycle CLASS,* Annals of Nuclear Energy (2015)
(6) D. Blanchet and al., *Sodium Fast Reactor Core Definition,* AEN-WPRS, OECD NEA (2011)
(7) P. Sciora and al*., Low void effect core design applied on 2400 MWth SFR reactor*, ICAPP (2011)
(8) W. Haeck and al., *Experimental validation of VESTA 2.1*, Joint International Conference on Supercomputing in Nuclear Applications and Monte Carlo (2013)
(9) LANL, *MCNP6 Users Manual - Code Version 6.1*, LA-CP-13-00634 (2013)
(10) S. Sala, *Réduction de la Radiotoxicité des Déchets Nucléaires à vie longue : Etudes Théoriques et Stratégiques de la Transmutation des Actinides Mineurs et des Produits de Fission dans les réacteurs électronucléaires*, Ph.D. Thesis in French, Université de Provence, France (1995)
(11) M.D. McKay and al., *Comparison of three methods for selecting values of input variables in the analysis of output from a computer code*, Technometrics 21 (1979)
(12) M. Ernoult and al., *Global and flexible models for sodium-cooled fast reactors in fuel cycle simulations*, PHYSOR (2018)
(13) A. Hoecker, and al., *TMVA: Toolkit for Multivariate Data Analysis*, CERN (2009)
(14) F. Courtin and al., *Neutronic predictors for PWR fuelled with multi-recycled plutonium and applications with the fuel cycle simulation tool CLASS*, Progress in Nuclear Energy (2017)